Journal of Hazardous Materials 162 (2009) 305–311

Contents lists available at ScienceDirect

Journal of Hazardous Materials

journal homepage: www.elsevier.com/locate/jhazmat

A novel agricultural waste adsorbent for the removal of cationic dye from aqueous solutions

B.H. Hameed*, R.R. Krishni, S.A. Sata

School of Chemical Engineering, Engineering Campus, Universiti Sains Malaysia, 14300 Nibong Tebal, Penang, Malaysia

ARTICLE INFO

Article history:
Received 12 January 2008
Received in revised form 7 May 2008
Accepted 8 May 2008
Available online 15 May 2008

Keywords:
Pineapple stem
Methylene blue
Adsorption isotherm
Equilibrium
Kinetic

ABSTRACT

In this paper, pineapple stem (PS) waste, an agricultural waste available in large quantity in Malaysia, was utilized as low-cost adsorbent to remove basic dye (methylene blue, MB) from aqueous solution by adsorption. Batch mode experiments were conducted at 30 °C to study the effects of initial concentration of methylene blue, contact time and pH on dye adsorption. Equilibrium adsorption isotherms and kinetic were investigated. The experimental data were analyzed by the Langmuir and Freundlich models and the isotherm data fitted well to the Langmuir isotherm with monolayer adsorption capacity of 119.05 mg/g. The kinetic data obtained at different concentrations were analyzed using a pseudo-first-order and pseudo-second-order equation and intraparticle diffusion equation. The experimental data fitted very well the pseudo-second-order kinetic model. The PS was found to be very effective adsorbent for MB adsorption.

1. Introduction

The textile dyeing industry consumes large quantities of water and produces large volumes of wastewater from different steps in the dyeing and finishing processes [1]. Though these release dyes into the environment constitute only a small proportion of water pollution, they are visible in small quantities due to their brilliance [2].

Many treatment processes have been applied for the removal of dyes from wastewater such as: photocatalytic degradation [3,4], sonochemical degradation [5], micellar enhanced ultrafiltration [6], cation exchange membranes [7], electrochemical degradation [8], adsorption/precipitation processes [9], integrated chemical–biological degradation [10], integrated iron(III) photoassisted-biological treatment [11], solar photo-Fenton and biological processes [12], Fenton-biological treatment scheme [13] and adsorption on activated carbon [14,15]. As synthetic dyes in wastewater cannot be efficiently decolorized by traditional methods, the adsorption of synthetic dyes on inexpensive and efficient solid supports was considered as a simple and economical method for their removal from water and wastewater [16].

The high cost of removal of dyes from aqueous solutions using adsorption on commercial activated carbons though very effective has motivated the search for alternatives adsorbents. Such alternatives include: waste metal hydroxide sludge [17], oil palm trunk fibre [18], broad bean peels [19], biomass fly ash [20], rice straw-derived char [21], durian (*Durio zibethinus* Murray) peel [22], chitosan bead [23], rice husk [24] and palm kernel fibre [25]. Recently, an extensive list of alternative and cheaper adsorbents for dyes removal has been compiled by Allen and Koumanova [26].

Pineapple (*Ananas comosus* Merr.) is the leading edible member of the family Bromeliaceae. It is a perennial plant with a height of 75–150 cm, a spread of 90–120 cm, a short, stout stump, and a rosette of long (50–180 cm), narrow, fibrous and spiny leaves [27]. According to the FAO online databases, it was estimated that Malaysia produced 255,000 T of pineapple in 2003 [28]. The pineapple is mainly produced as canned fruits and consumed worldwide [28]. The crown leaves and stems are the burden of the canned pineapple industry because the need of these leaves for replanting is relatively small compared to the amount of the refuse generated, thus become an issue and contributes to serious environmental problems. Therefore, to help in the disposal of these wastes, a study could be carried out on the possibility of converting these wastes into a profitable adventure; which formed the motivations of this present study.

The main aim of this study was to investigate the potentiality of using pineapple stem (PS) as an adsorbent for the adsorption of methylene blue (MB). The effects of initial dye concentration, contact time and pH on MB adsorption were studied. Adsorption isotherms and kinetics parameters were also calculated and discussed.

* Corresponding author. Fax: +60 4 594 1013.
E-mail address: chbassim@eng.usm.my (B.H. Hameed).

0304-3894/$ – see front matter © 2008 Elsevier B.V. All rights reserved.
doi:10.1016/j.jhazmat.2008.05.036

2. Material and methods

2.1. Adsorbate

Basic dye used in this study was methylene blue purchased from Sigma–Aldrich. MB has molecular formula $C_{16}H_{18}N_3ClS$ (Mol. wt. 319.85 g/mol). The maximum wavelength of this dye is 668 nm. The dye stock solution was prepared by dissolving accurately weight dye in distilled water to the concentration of 1 g/L. The experimental solutions were obtained by diluting the dye stock solution in accurate proportions to needed initial concentrations.

2.2. Preparation of adsorbent

Pineapple stems were collected from nearby market as solid waste. The collected materials were then washed with distilled water for several times to remove all the dirt particles. The washed materials were cut into small pieces (1–3 cm) and dried in a hot air oven at 70 °C for 48 h. Then ground and finally screened to obtain a particle size range of 355–500 μm. Thirty grams of PS was repeatedly washed with hot distilled water until the filtered water was clear. Therefore, the PS was dried at 70 °C for 24 h in an oven and then stored in plastic bottles for further use.

2.3. Scanning electron microscopy and Fourier Transform Infra Red study

Scanning electron microscopy (SEM) analysis was carried out on the PS to study its surface texture before and after MB adsorption. Fourier Transform Infrared.

(FTIR) (FTIR-2000, PerkinElmer) analysis was applied on the unused PS and dye-adsorbed-PS to determine the surface functional groups, and the spectra were recorded from 4000 to 400 cm^{-1}.

2.4. Equilibrium studies

A fixed amount of adsorbent (0.30 g) was added into a set of each 250 mL Erlenmeyer flasks containing 200 mL of different initial concentrations (25, 50, 100, 150, 200, 250 and 300 mg/L) of dye solution without adjusting pH. The flaks were agitated in an isothermal water bath shaker at 120 rpm and 30 °C for 5 h and 30 min until equilibrium was reached. At time $t = 0$ and equilibrium, the dye concentration were measured by a double beam UV/Vis spectrophotometer (Shimadzu, Model UV 1601, Japan) at 668 nm. Each experiment was duplicated under identical conditions. The amount of adsorption at equilibrium, q_e (mg/g), was calculated by:

$$q_e = \frac{(C_0 - C_e)V}{W} \quad (1)$$

where C_0 and C_e (mg/L) are the liquid-phase concentrations of dye at initial and equilibrium time t, respectively. V (L) is the volume of the solution, and W (g) is the mass of adsorbent used.

The dye removal percentage can be calculated as follows:

$$\text{Removal percentage} = \left(\frac{C_0 - C_t}{C_0}\right) \times 100 \quad (2)$$

where C_t (mg/L) is the liquid-phase concentrations of dye at time t.

2.5. Effect of pH

The effect of pH on the amount of dye removal was studied over the pH range from 2 to 10. The pH was adjusted by adding a few drops of 1.0N NaOH or 1.0N HCl. In this study, 200 mL of a fixed initial concentration of dye solution at different pH were agitated with 0.30 g of PS adsorbent using water-bath shaker at 30 °C. Agitation was provided at a constant speed of 120 rpm for 5 h 30 min. The concentrations at equilibrium were determined.

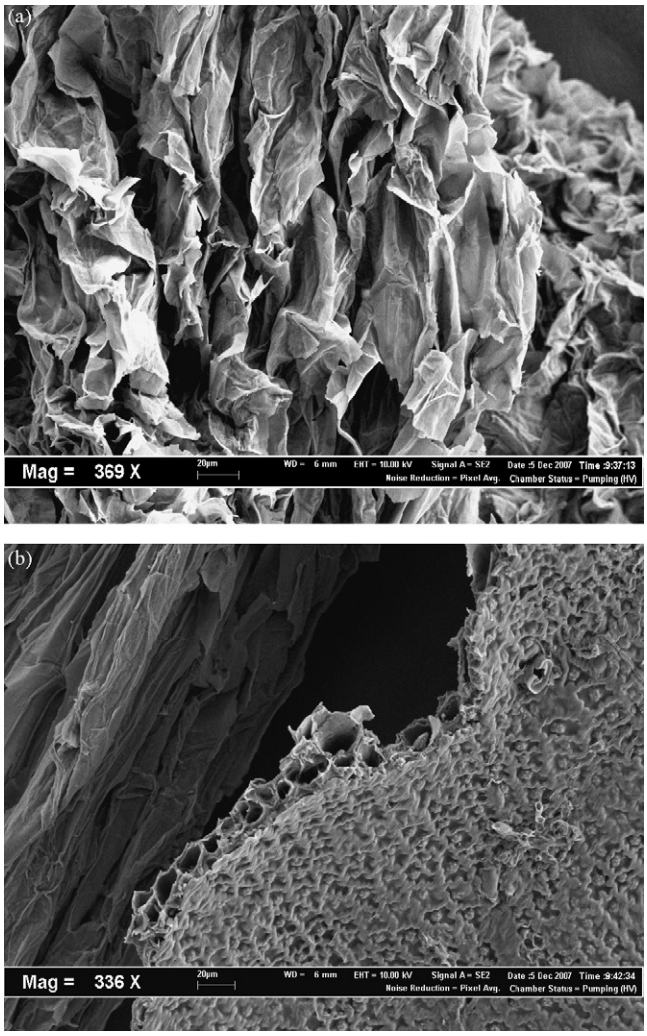

Fig. 1. SEM micrographs of PS particle (a) before dye sorption (magnification: 369) and (b) with dye adsorbed (magnification: 336).

2.6. Batch kinetic studies

The procedure of kinetic tests was identical to those of equilibrium tests. The aqueous samples were taken at preset time intervals and the concentrations of MB solutions were similarly measured. The amount of adsorption at time t, q_t (mg/g), was calculated by:

$$q_t = \frac{(C_0 - C_t)V}{W} \quad (3)$$

3. Results and discussion

3.1. SEM and FTIR of PS

Fig. 1 shows the SEM micrographs of PS sample before and after dye adsorption. It is clear that PS has considerable numbers of heterogeneous layer of pores where there is a good possibility for dye to be adsorbed. The surface of dye-loaded adsorbent, however, clearly shows that the surface of PS is covered with dye molecules (Fig. 1b).

The FTIR spectrum of PS (Fig. 2 and Table 1) shows that some peaks were shifted or disappeared and that new peaks were also

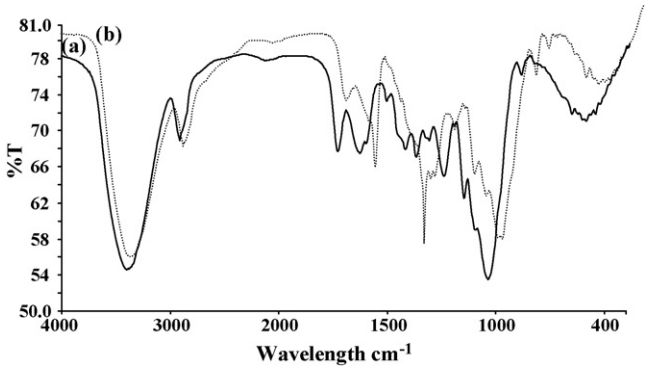

Fig. 2. FTIR of PS adsorbent: (a) before dye sorption and (b) after dye adsorption.

detected. These changes observed in the spectrum indicated the possible involvement of those functional groups on the surface of the PS in adsorption process.

3.2. Effect of contact time and initial dye concentration

The effect of the initial MB concentration on the MB adsorption by PS is shown in Fig. 3. It can be seen that the amount of dye adsorbed (mg/g) increased with increased dye concentration and remained constant after equilibrium time. The concentration provides an important driving force to overcome all mass transfer resistance of the dye between the aqueous and solid phases. Hence a higher initial concentration of dye will enhance the adsorption process. The equilibrium sorption capacity of the PS increased with an increase initial dye concentration, while the % removal of dye showed the opposite trend. When the initial dye concentration increased from 25 to 300 mg/L, the loading capacity of PS increased from 18.33 to 116.95 mg/g and the percentage removal decreased from 96.70 to 54.50%. A similar trend was also observed for MB adsorption onto *Parthenium hysterophorus* [29] and MB onto bamboo-based activated carbon [30].

Fig. 3 also indicated that the contact time needed for MB solutions with initial concentrations of 25–100 mg/L to reach equilibrium was less than 1 h and 30 min. For MB solutions with initial concentrations of 150–300 mg/L, equilibrium time of 4 h was required. However, the experimental data were measured at 5 h and 30 min to be sure that full equilibrium was attained. A similar observation was reported for the adsorption of MB on pomelo (*Citrus grandis*) peel [24].

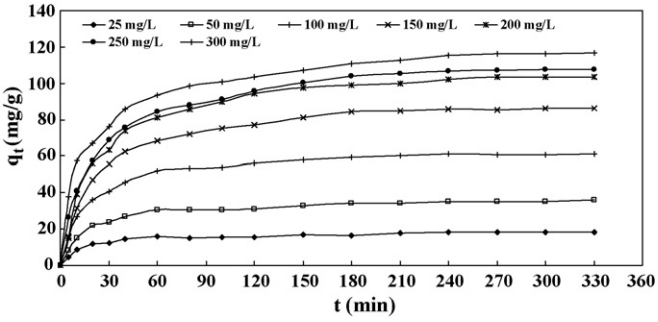

Fig. 3. Effect of initial concentration on removal of MB by PS (conditions: W = 0.30 g/200 mL; temperature = 30 °C).

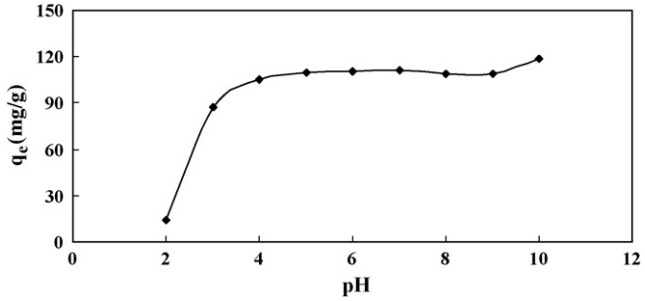

Fig. 4. Effect of the solution pH on the adsorption of MB on PS (C_0 = 250 mg/L, temperature 30 °C, agitation rate 120 rpm and W = 0.3 g).

3.3. Effect of solution pH on dye adsorption

The effect of solution pH on the equilibrium up-take capacity of PS was studied at 250 mg/L initial dye concentration and temperature 30 °C between pH value of 2 and 10. As shown in Fig. 4, the dye up-take was found to increase with an increase in pH. It increased from 13.29 to 104.50 mg/g for an increase in pH from 2 to 10. A consistent increase in adsorption capacity of the PS was noticed as the pH increased from 2 to 4, but further increase in pH from 4 to 9 seemed not affect the sorption in any wise. A similar trend was reported for the adsorption of MB onto wheat shells [31].

Table 1
FTIR of PS adsorbent

IR peak	Frequency (cm^{-1})		Differences	Assignment
	Before adsorption	After adsorption		
1	3,402	3,398	4	Bonded —OH groups
2	2,919	2,916	3	Two bands for—CH_2—groups
3	2,130	–		C=N stretching
4	1,736	1,733	3	C=O stretching
5	1,635	–		C=O stretching
6	1,605	1,602	3	Bonded C=C
7	1,513	–		NH stretching
8	1,427	–		in-plane —OH bending and C—O stretch of dimmers
9	1,377	1,384	−7	CH_3 deformation
10	1,318	1,355	−37	—NO_2 aromatic nitro compounds
11	–	1,337		SO_2—NH_2 sulfonamides
12	1,252	1,248	4	C—O stretching
13	1,159	1,161	−2	C—N stretching
14	–	1,107		—C—NH_3 primary aliphatic amines
15	1,048	1,037	11	P—O—C strongest band highest frequencies for aliphatic amines
16	896	886	10	CH out-of-plane deformation
17	–	828,791		CH out-of-plane deformation
18	667	664	3	C—O—H twist broad

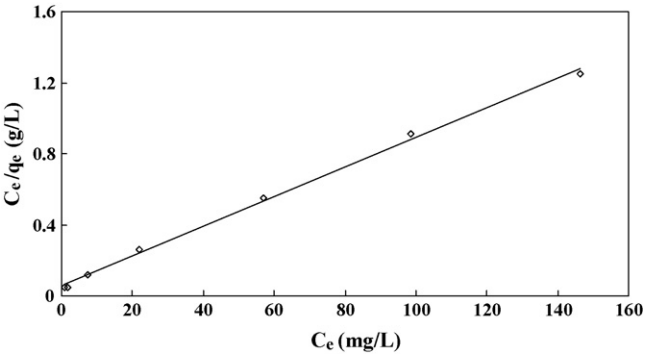

Fig. 5. Langmuir isotherm for MB sorption onto PS.

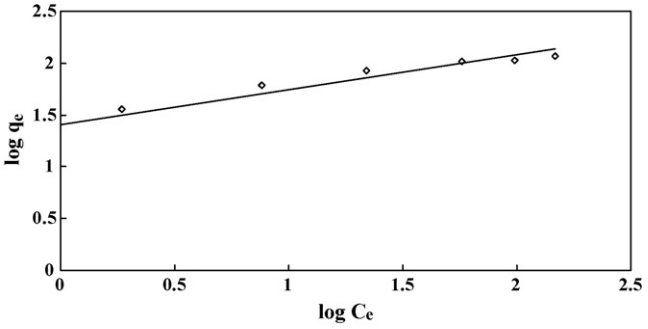

Fig. 6. Freundlich isotherm for MB sorption onto PS.

At lower pH as 2, the surface charge may be positively charged, thus making (H^+) ions compete effectively with dye cations causing a decrease in the amount of dye adsorbed. At higher pH the surface of PS, may be negatively charged which enhance the positively charged dye cations through electrostatic force at attraction [32]. A similar trend was also observed for adsorption of MB onto beech sawdust [33] and malachite green onto treated sawdust [21]. Present result is in good agreements with the above previous findings.

3.4. Adsorption isotherms

In order to establish the most appropriate correlations for the equilibrium data in the design of adsorption system, two common isotherm models were tested: the Langmuir and Freundlich models. The applicability of the isotherm equations was compared by judging the correlation coefficients, R^2.

The Langmuir adsorption [34] model is based on the assumption that maximum adsorption corresponds to a saturated monolayer of solute molecules on the adsorbent surface. The linear form of the Langmuir equation can be described by

$$\frac{C_e}{q_e} = \left(\frac{1}{Q_0 b}\right) + \left(\frac{1}{Q_0}\right) C_e \quad (4)$$

where C_e (mg/L) is the equilibrium concentration of the adsorbate, q_e (mg/g) is the amount of adsorbate per unit mass of adsorbent, Q_0 and b are Langmuir constants related to adsorption capacity and rate of adsorption, respectively. The linear plot of specific adsorption (C_e/q_e) against the equilibrium concentration (C_e) (Fig. 5) shows that the adsorption obeys the Langmuir model. The Langmuir constants Q_0 and b were determined from the slope and intercept of the plot and are presented in Table 2. The R^2 values (0.998) suggest that the Langmuir isotherm provides a good fit to the isotherm data. A similar observation was reported for adsorption of MB on fly ash [35], pomelo (*Citrus grandis*) [24], silk worm [36], cedar sawdust and crushed brick [37].

Table 2
Langmuir and Freundlich isotherm constants and correlation coefficients for adsorption of MB onto PS adsorbent

Langmuir isotherm	
Q_0	119.05
b	0.00009
R^2	0.998
Freundlich isotherm	
K_F	25.42
n	2.97
R^2	0.921

The essential characteristics of the Langmuir isotherm can be expressed in terms of a dimensionless constant separation factor R_L [38] given by Eq. (5)

$$R_L = \frac{1}{1 + bC_0} \quad (5)$$

where C_0 (mg/L) is the highest initial concentration of adsorbent, and b (L/mg) is Langmuir constant. The parameter R_L indicates the nature of shape of the isotherm accordingly:

$R_L > 1$	Unfavorable adsorption
$0 < R_L < 1$	Favorable adsorption
$R_L = 0$	Irreversible adsorption
$R_L = 1$	Linear adsorption

The value of R_L in the present investigation has been found to be 0.9737 at 30 °C showing that the adsorption of MB on PS is favorable at the temperature studied.

The Freundlich isotherm [39] is the earliest known relationship describing the sorption equation. The fairly satisfactory empirical isotherm can be used for non-ideal sorption that involves heterogeneous surface energy systems and is expressed by the following equation:

$$q_e = K_F C_e^{1/n} \quad (6)$$

where K_F (mg/g (L/mg)$^{1/n}$) is roughly an indicator of the adsorption capacity and $1/n$ is the adsorption intensity. In general, as the K_F value increases the adsorption capacity of adsorbent for a given adsorbate increases. The magnitude of the exponent, $1/n$ gives an indication of the favorability of adsorption. Value of $n > 1$ represents favorable adsorption condition [40,41]. The linear form of Eq. (6) is:

$$\log q_e = \log K_F + \left(\frac{1}{n}\right) \log C_e \quad (7)$$

Values of K_F and n are calculated from the intercept and slope of the plot (Fig. 6) and are listed in Table 2.The R^2 value (0.921) is lower than Langmuir isotherm. The value of Freundlich exponent n (2.97) is the range of $n > 1$, indicating a favorable adsorption [40,41].

The best equilibrium model was determined based on the linear square regression correlation coefficient R^2. From Table 2, it was observed that the equilibrium sorption data were very best represented by the Langmuir isotherm. The best fit isotherm expressions confirm the monolayer coverage process of MB onto PS. A similar result was reported for adsorption of methylene blue on adsorbents materials produce from sewage sludge [42].

Table 3 lists a comparison of maximum monolayer adsorption capacity of MB on various adsorbents. PS is found to have a relatively large adsorption capacity of 119.05 mg/g and this indicates that it could be considered a promising material for the removal basic dye from aqueous solution, mostly when compared with waste apricot

Table 3
Comparison of adsorption capacities of various adsorbents for MB

Adsorbent	Q_0 (mg/g)	T (°C)	Reference
Pineapple stem	119.05	30	This study
Sulfuric acid treated Parthenium (SWC)	88.29	26 ± 1	[29]
Pathenium (PWC)	20.8	30	[29]
Wheat shells	16.56	30	[31]
Raw *Posidonia oceanica* fibres	5.56	30	[32]
Yellow passion fruit peel	0.0068	25	[33]
Cedar sawdust	142.36	20	[36]
Crushed brick	96.61	20	[36]
Waste apricot-based activated carbon	102.04–136.98	30–50	[43]
Bamboo dust carbon	143.20	30	[44]
Dehydrated peanut hull	123.5	27	[45]
Rice husk	40.58	32	[46]
Orange peel	18.6	30	[47]
Eggshell	0.80	25	[48]
Eggshell membrane	0.24	25	[48]

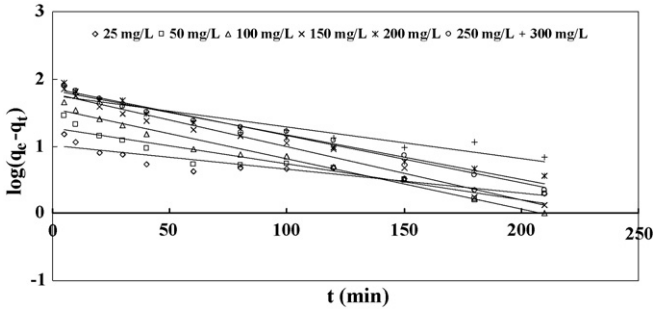

Fig. 7. Pseudo-first-order kinetics for adsorption of MB on PS.

based activated carbon (102.04–136.98 mg/g) [44] and dehydrated peanut hull (123.5 mg/g) [46].

3.5. Adsorption kinetics

Pseudo-first-order and second-order models were applied to test experimental data and thus elucidated the kinetic adsorption process. Lagergren proposed a method for adsorption analysis which is the pseudo-first-order kinetic equation of Lagergren [49] in the form:

$$\log(q_e - q_t) = \log q_e - \frac{k_1}{2.303} t \quad (8)$$

where k_1 (1/min), is the rate constant, q_e (mg/g) is the amount of solute adsorbed on the surface at equilibrium and q_t (mg/g) is the amount of solute adsorbed at any time. The value of k_1 for MB adsorption by PS was determined from the plot of $\log(q_e - q_t)$ against t (Fig. 7). The parameters of pseudo-first-order model are summarized in Table 4.

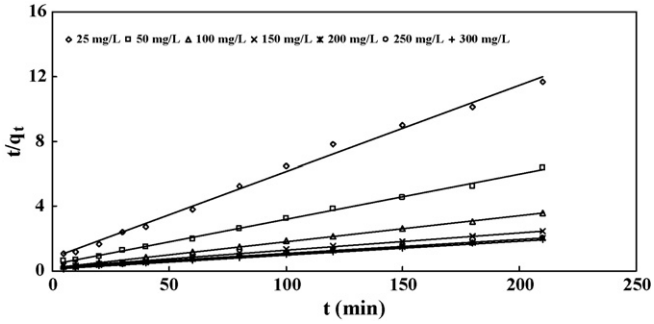

Fig. 8. Pseudo-second-order kinetics for adsorption of MB on PS.

Although the correlation coefficients (R^2) are generally greater than 0.858 for all initial concentrations under the limit of the experimental q_e for the pseudo-first-order kinetic model. As such, the adsorption of MB on PS cannot be best described by the pseudo-first-order kinetic. In many cases the first-order equation of Lagergren does not fit well to the whole range of contact time and is generally applicable over the initial stage of the adsorption processes [50]. Therefore, the pseudo-second-order kinetic model [41,51] as shown in Eq. (9) was used to study the adsorption kinetic of the present system.

$$\frac{t}{q_t} = \frac{1}{k_2 q_e^2} + \left(\frac{1}{q_e}\right) t \quad (9)$$

where k_2 (g/mg min) is the second-order rate constant. The q_e and k_2 can be calculated from the slope and intercept of the plots t/q_t versus t (Fig. 8).

The constant k_2 is used to calculate the initial sorption rate h (mg/g min), as $t \to 0$ as follows:

$$h = k_2 q_e^2 \quad (10)$$

The pseudo-second-order rate constants k_2, the calculated h values, and the corresponding linear regression correlation coefficients R^2 are given in Table 4. The R^2 values were found to be in the range 0.994–1.000. Moreover, the variations between the calculated q_e and experimental q_e were very minimal for this model.

The high correlations coefficient and high agreement that exist between the calculated and experimental q_e values of the pseudo-second-order kinetic model over the other model renders it best in adsorption of MB on PS. This confirms that the sorption data are well represented by the pseudo-second-order kinetics for the entire sorption period. The increase in values of the initial adsorption rates, h (Table 4) with an increase in the initial dye concentration could be attributed to the increase in the driving force for mass transfer, allowing more dye molecules to reach the surface of the adsorbents in a shorter period of time [52,53].

The kinetic results were further analyzed by the intraparticle diffusion model to elucidate the diffusion mechanism [54]:

$$q_t = k_{id} t^{1/2} + C \quad (11)$$

Table 4
Comparison of the pseudo-first-order, pseudo-second-order adsorption rate constant and calculated and experimental q_e value obtained at different initial MB concentrations

C_0 (mg/L)	Pseudo-first-order kinetic model				Pseudo-second-order kinetic model			
	$q_{e,exp}$ (mg/g)	$q_{e,cal}$ (mg/g)	k_1 (1/min)	R^2	$q_{e,cal}$ (mg/g)	k_2 (g/mg min)	R^2	h (mg/g min)
25	20.00	10.19	0.0081	0.858	18.73	0.0036	0.994	1.263
50	36.00	18.55	0.0122	0.900	35.97	0.0019	0.998	2.458
100	60.92	35.65	0.0170	0.977	62.50	0.0013	0.996	5.078
150	86.03	60.81	0.0182	0.979	93.46	0.0005	1.000	4.367
200	103.64	67.87	0.0152	0.971	114.94	0.0004	0.998	8.403
250	107.72	72.53	0.0161	0.987	133.64	0.0003	0.998	5.359
300	116.95	56.18	0.0108	0.905	114.94	0.0007	0.999	9.248

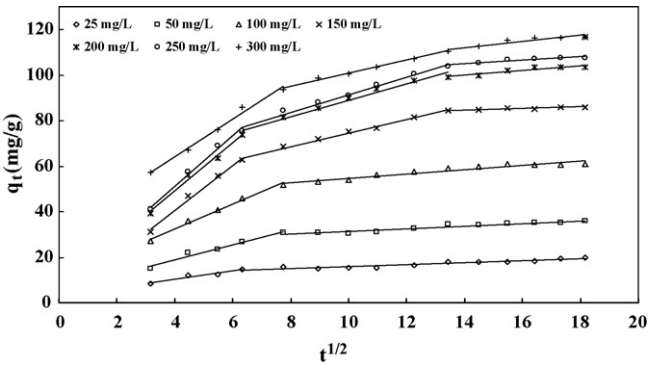

Fig. 9. Intraparticle diffusion constants for different initial MB dye concentrations.

where C is the intercept and k_{id} is the intraparticle diffusion rate constant (mg/g min$^{0.5}$), which can be evaluated from the slope of the linear plot of q_t versus $t^{1/2}$ (Fig. 9). If the regression of q_t versus $t^{1/2}$ is linear and passes through the origin, then intraparticle diffusion is the sole rate-limiting step [55]. For intraparticle diffusion plots, the first, sharper region is the instantaneous adsorption or external surface adsorption. The second region is the gradual adsorption stage where intraparticle diffusion is the rate limiting. In some cases, the third region exists, which is the final equilibrium stage where intraparticle diffusion starts to slow down due to the extremely low adsorbate concentrations left in the solutions [56]. As seen from Fig. 9, the plots were not linear over the whole time range, implying that more than one process affected the adsorption.

4. Conclusions

The results revealed the potential of pineapple stem, an agricultural waste material, to be a low-cost adsorbent for removing basic dye from aqueous solutions. Equilibrium data agreed well with Langmuir isotherm model with monolayer adsorption capacity of 119.05 mg/g at 30 °C. The value of the separation factor, R_L, indicated the dye/PS system was a favorable adsorption. The suitability of pseudo-first-order kinetic and pseudo-second-order kinetic models for the sorption of MB onto PS was also discussed. The kinetic modeling study has shown that the experimental data were found to follow the pseudo-second-order model suggesting a chemisorption process.

Acknowledgment

The authors acknowledge the research grant provided by the University Science Malaysia under the Research University (RU) Scheme (Project No: 1001/PJKIMIA/814005).

References

[1] B. Ramesh Babu, A.K. Parande, S. Raghu, T. Prem Kumar, Cotton textile processing: waste generation and effluent treatment, J. Cotton Sci. 11 (2007) 141–153.
[2] T. Robinson, G. McMullan, R. Marchant, P. Nigam, Remediation of dyes in textile effluent: a critical review on current treatment technologies with a proposed alternative, Bioresour. Technol. 77 (2001) 247–255.
[3] M.R. Sohrabi, M. Ghavami, Photocatalytic degradation of Direct Red 23 dye using UV/TiO_2: effect of operational parameters, J. Hazard. Mater. 153 (2008) 1235–1239.
[4] M. Sleiman, D.L Vildozo, C. Ferronato, J.M. Chovelon, Photocatalytic degradation of azo dye Metanil Yellow: optimization and kinetic modeling using a chemometric approach, Appl. Catal. B: Environ. 77 (2007) 1–11.
[5] M. Abbasi, N.R. Asl, Sonochemical degradation of Basic Blue 41 dye assisted by nanoTiO_2 and H_2O_2, J. Hazard. Mater. 153 (2008) 942–947.
[6] N. Zaghbani, A. Hafiane, M. Dhahbi, Removal of Safranin T from wastewater using micellar enhanced ultrafiltration, Desalination 222 (2008) 348–356.
[7] J.S. Wu, C.H. Liu, K.H. Chu, S.Y. Suen, Removal of cationic dye methyl violet 2B from water by cation exchange membranes, J. Membr. Sci. 309 (2008) 239–245.
[8] L. Fan, Y. Zhou, W. Yang, G. Chen, F. Yang, Electrochemical degradation of aqueous solution of Amaranth azo dye on ACF under potentiostatic model, Dyes Pigments 76 (2008) 440–446.
[9] M.X. Zhu, L. Lee, H.H. Wang, Z. Wang, Removal of an anionic dye by adsorption/precipitation processes using alkaline white mud, J. Hazard. Mater. 149 (2007) 735–741.
[10] G. Sudarjanto, B. Keller-Lehmann, J. Keller, Optimization of integrated chemical–biological degradation of a reactive azo dye using response surface methodology, J. Hazard. Mater. 138 (2006) 160–168.
[11] V. Sarria, M. Deront, P. Péringer, C. Pulgarin, Degradation of a biorecalcitrant dye precursor present in industrial wastewaters by a new integrated iron(III) photoassisted-biological treatment, Appl. Catal. B: Environ. 40 (2003) 231–246.
[12] J. García-Montaño, L. Pérez-Estrada, I. Oller, M.I. Maldonado, F. Torrades, J. Peral, Pilot plant scale reactive dyes degradation by solar photo-Fenton and biological processes, J. Photochem. Photobiol. A: Chem. 195 (2008) 205–214.
[13] B. Lodha, S. Chaudhari, Optimization of Fenton-biological treatment scheme for the treatment of aqueous dye solutions, J. Hazard. Mater. 148 (2007) 459–466.
[14] B.H. Hameed, F.B.M. Daud, Adsorption studies of basic dye on activated carbon derived from agricultural waste: Hevea brasiliensis seed coat, Chem. Eng. J. 139 (2008) 48–55.
[15] F.C. Wu, R.L. Tseng, High adsorption capacity NaOH-activated carbon for dye removal from aqueous solution, J. Hazard. Mater. 152 (2008) 1256–1267.
[16] E. Forgacs, T. Cserháti, G. Oros, Removal of synthetic dyes from wastewaters: a review, Environ. Int. 30 (2004) 953–971.
[17] S.C.R. Santos, V.J.P. Vilar, R.A.R. Boaventura, Waste metal hydroxide sludge as adsorbent for a reactive dye, J. Hazard. Mater. 153 (2008) 999–1008.
[18] B.H. Hameed, M.I. El-Khaiary, Batch removal of malachite green from aqueous solutions by adsorption on oil palm trunk fibre: equilibrium isotherms and kinetic studies, J. Hazard. Mater. 154 (2008) 237–244.
[19] B.H. Hameed, M.I. El-Khaiary, Sorption kinetics and isotherm studies of a cationic dye using agricultural waste: broad bean peels, J. Hazard. Mater. 154 (2008) 639–648.
[20] P. Pengthamkeerati, T. Satapanajaru, O. Singchan, Sorption of reactive dye from aqueous solution on biomass fly ash, J. Hazard. Mater. 153 (2008) 1149–1156.
[21] B.H. Hameed, M.I. El-Khaiary, Kinetics and equilibrium studies of malachite green adsorption on rice straw-derived char, J. Hazard. Mater. 153 (2008) 701–708.
[22] B.H. Hameed, H. Hakimi, Utilization of durian (*Durio zibethinus* Murray) peel as low cost sorbent for the removal of acid dye from aqueous solutions, Biochem. Eng. J. 39 (2008) 338–343.
[23] Z. Bekçi, C. Özveri, Y. Seki, K. Yurdakoç, Sorption of malachite green on chitosan bead, J. Hazard. Mater. 154 (2008) 254–261.
[24] R. Han, D. Ding, Y. Xu, W. Zou, Y. Wang, Y. Li, L. Zou, Use of rice husk for the adsorption of congo red from aqueous solution in column mode, Bioresour. Technol. 99 (2008) 2938–2946.
[25] A.E. Ofomaja, Y.S. Ho, Equilibrium sorption of anionic dye from aqueous solution by palm kernel fibre as sorbent, Dyes Pigments 74 (2007) 60–66.
[26] S.J. Allen, B. Koumanova, Decolourisation of water/wastewater using adsorption, J. Univ. Chem. Technol. Metall. 40 (2005) 175–192.
[27] J. Morton, Pineapple, in: J.F. Morton (Ed.), Fruits of Warm Climates, Miami, FL, 1987, pp. 18–28.
[28] A.V. Tran, Chemical analysis and pulping study of pineapple crown leaves, Ind. Crops Prod. 24 (2006) 66–74.
[29] H. Lata, V.K. Grag, R.K. Gupta, Removal of a basic dye from aqueous solution by adsorption using *Parthenium hysterophorus*: an agricultural waste, Dyes Pigments 74 (2007) 653–658.
[30] B.H. Hameed, A.T.M. Din, A.L. Ahmad, Adsorption of methylene blue onto bamboo-based activated carbon: kinetics and equilibrium studies, J. Hazard. Mater. 141 (2007) 819–825.
[31] Y. Bulut, H. Aydin, A kinetics and thermodynamics study of methylene blue adsorption on wheat shells, Desalination 194 (2006) 259–267.
[32] M.C. Ncibi, B. Mahjoub, M. Seffen, Kinetic and equilibrium studies of methylene blue biosorption by *Posidonia oceanica* (L.) fibres, J. Hazard. Mater. 139 (2007) 280–285.
[33] F.A. Pavan, A.C. Mazzocato, Y. Gushiken, Removal of Methylene blue dye from aqueous solutions by adsorption using yellow passion fruit peel as adsorbent, Bioresour. Technol. 99 (2008) 3162–3165.
[34] I. Langmuir, The adsorption of gases on plane surfaces of glass, mica and platinum, J. Am. Chem. 57 (1918) 1361–1403.
[35] K. Vasanth Kumar, V. Ramamurthi, S. Sivanesan, Modeling the mechanism involved during the sorption of methylene blue fly ash, J. Colloid Interface Sci. 284 (2005) 14–21.
[36] B. Noroozi, G.A. Sorial, H. Bahrami, M. Arami, Equilibrium kinetics adsorption study of a cationic dye by a natural adsorbent—Silkworm pupa, J. Hazard. Mater. 139 (2007) 167–174.
[37] Q. Hamdaoui, Batch study of liquid-phase adsorption of methylene blue using cedar sawdust and crushed brick, J. Hazard. Mater. 135 (2006) 264–273.
[38] H.R. Hall, L.C. Eagleton, A. Acrivos, T. Vermeulen, Pore- and solid-diffusion kinetics in fixed-bed adsorption under constant-pattern conditions, I&EC Fundam. 5 (1966) 212–223.
[39] H. Freundlich, Über die adsorption in lösungen (adsorption in solution), Z. Phys. Chem. 57 (1906) 384–470.

[40] R.E. Treybal, Mass Transfer Operations, second ed., McGraw Hill, New York, 1968.
[41] Y.S. Ho, G. McKay, Sorption of dye from aqueous solution by peat, Chem. Eng. J. 70 (1998) 115–124.
[42] M. Otero, F. Rozada, L.F. Calvo, A.I. García, A. Morán, Kinetic and equilibrium modelling of the methylene blue removal from solution by adsorbent materials produced from sewage sludges, Biochem. Eng. J. 15 (2003) 59–68.
[43] C.A. Başar, Applicability of the various adsorption models of three dyes adsorption onto activated carbon prepared waste apricot, J. Hazard. Mater. 135 (2006) 232–241.
[44] N. Kannan, M.M. Sundaram, Kinetics and Mechanism of removal of methylene blue by adsorption on various carbon-comparative study, Dyes Pigments 51 (2001) 25–40.
[45] D. Özer, G. Dursun, A. Özer, Methylene blue adsorption from aqueous solution by dehydrated peanut hull, J. Hazard. Mater. 144 (2007) 171–179.
[46] V. Vadivelan, K.V. Kumar, Equilibrium, kinetics, mechanism, and process design for the sorption of methylene blue onto rice husk, J. Colloid Interface Sci. 286 (2005) 90–100.
[47] G. Annadurai, R.S. Juang, D.J. Lee, Use of cellulose-based wastes for adsorption of dyes from aqueous solutions, J. Hazard. Mater. B92 (2002) 263–274.
[48] W.T. Tsai, J.M. Yang, C.W. Lai, Y.H. Cheng, C.C. Lin, C.W. Yeh, Characterization and adsorption properties of eggshells and eggshell membrane, Bioresour. Technol. 97 (2006) 488–493.
[49] S. Langergren, About the theory of so-called adsorption of soluble substances, Kungliga Svenska Vetenskapsakademies Handlingar 24 (4) (1898) 1–39.
[50] Y.S. Ho, G. McKay, A comparison of chemisorption kinetic models applied to pollutant removal on various sorbents, Process Saf. Environ. Prot. 76 (B4) (1998) 332–340.
[51] Y.S. Ho, G. McKay, The kinetics of sorption of divalent metal ions onto sphagnum moss peat, Water Res. 34 (2000) 735–742.
[52] Y.S. Ho, G. McKay, Kinetic models for the sorption of dye from aqueous solution by wood, Process Saf. Environ. Prot. 76 (B2) (1998) 183–191.
[53] Y.S. Ho, G. McKay, Kinetic model for lead(II) sorption on to peat, Adsorpt. Sci. Technol. 16 (4) (1998) 243–255.
[54] W.J. Weber Jr., J.C. Morris, Kinetics of adsorption on carbon from solution, J. Sanitary Eng. Div. Am. Soc., Civ. Eng. 89 (1963) 31–60.
[55] V.J.P. Poots, G. McKay, J.J. Healy, The removal of acid dye from effluent using natural adsorbents: I. Peat, Water Res. 10 (12) (1976) 1061–1066.
[56] W.H. Cheung, Y.S. Szeto, G. McKay, Intraparticle diffusion processes during acid dye adsorption onto chitosan, Bioresour. Technol. 98 (2007) 2897–2904.